Inorganic Chemistry

Article

pubs.acs.org/IC

Redox Noninnocence in Coordinated 2-(Arylazo)pyridines: Steric Control of Ligand-Based Redox Processes in Cobalt Complexes

Pradip Ghosh,[†] Subhas Samanta,[†] Suman K Roy,[†] Sucheta Joy,[†] Tobias Krämer,[‡] John E. McGrady,*[,‡] and Sreebrata Goswami*[,†]

[†]Department of Inorganic Chemistry, Indian Association for the Cultivation of Science, Kolkata 700 032, India

[‡]Inorganic Chemistry Laboratory, Department of Chemistry, University of Oxford, South Parks Road, Oxford OX1 3QR, U.K.

Supporting Information

ABSTRACT: A series of cobalt complexes of ligands based on the 2-(arylazo)pyridine architecture have been synthesized, and the precise structure and stoichiometry of the complexes depend critically on the identity of substituents in the 2, 4, and 6 positions of the phenyl ring. The 2-(arylazo)pyridine motif can support either Co^{II} complexes with neutral ligands, $Co^{II}Cl_2(L^a)_2$ (**1**), $Co^{II}Cl_2(L^c)_2$ (**3**), $[Co^{II}Cl(L^b)_2]_2(PF_6)_2$ (**5**$[PF_6]_2$), or Co^{III} complexes of reduced 2-(arylazo)pyridine ligand radical anions, $L^{\bullet-}$, $Co^{III}Cl(L^{b\bullet-})_2$ (**2**), $Co^{III}Cl(L^{c\bullet-})_2$ (**4**), and $Co^{III}Me(L^{b\bullet-})_2$ (**6**). All three members of the latter class are based on approximately trigonal-bipyramidal $CoX(L^{\bullet-})_2$ architectures [L = 2-(arylazo)pyridine] with two azo nitrogen atoms and the X ligand (X = Cl or Me) in the equatorial plane and two pyridine nitrogen atoms occupying axial positions. Density functional theory suggests that the electronic structure of the Co^{III} complexes is also dependent on the identity of X: the strong σ-donor methyl gives a low-spin (S = 0) configuration, while the σ/π-donor chloro gives an intermediate-spin (S = 1) local configuration. In certain cases, one-electron reduction of the $Co^{II}X_2L_2$ complex leads to the formation of $Co^{III}X(L^{\bullet-})_2$; i.e., reduction of one ligand induces a further one-electron oxidation of the metal center with concomitant reduction of the second ligand.

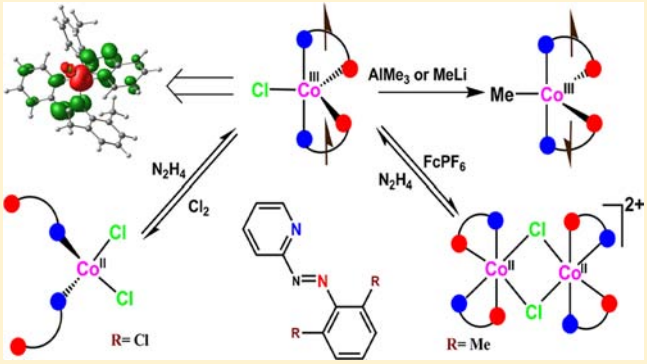

INTRODUCTION

The majority of studies of the redox properties of coordination complexes have focused on the metal ion, with the surrounding ligands generally being regarded as mere spectators. However, the concept of ligand "noninnocence",[1] wherein a ligand, rather than the metal center, is the site of redox activity, has been appreciated for almost half a century. A number of practical applications of transition metal−ligand radical complexes in catalytic and enzymatic processes have also emerged,[2−9] and the synergy between metal and ligand redox has been the subject of a recent review.[10] Among these families of redox noninnocent ligands, the azoanion-radical complexes have long been known in solution,[11] although X-ray structural authentication first appeared only in the late 1990s with complexes of two neutral azoaromatic ligands.[12,13] In the past decade, a number of metal complexes of azoanion-radical ligands have emerged,[14−16] primarily as a result of ligand-based unusual redox chemistry. Herein we report several Co^{II} and Co^{III} complexes of 2-(phenylazo)pyridine and its derivatives and their associated redox chemistry. The ligands vary in their substituents at the two *o*-carbon atoms of the phenyl ring, which impart significant differences in steric crowding in the coordination sphere. The complexes are characterized by X-ray crystallography, electrochemistry, and spectroscopy, and a detailed electronic structure analysis using density functional theory (DFT) is also reported. The structural differences prove to be intimately related to the oxidation level of the ligand.

RESULTS AND DISCUSSION

Chemical Reactions. The work begins with three separate chemical reactions of three very similar ligands, L^{a-c}, with hydrated $Co^{II}Cl_2$ in 2:1 molar proportions in a methanol solvent. The ligands are based on the 2-(arylazo)pyridine architecture but differ in the identity of the substituents in the ortho (R) and para (Y) positions. These are shown in Chart 1, and their chemical reactions are summarized in Scheme 1.

The reactions lead to the isolation of three quite different complexes, **1**−**3**, each in near-quantitative yield: (i) octahedral $CoCl_2(L^a)_2$ (brown, **1**); (ii) distorted trigonal-bipyramidal $CoCl(L^b)_2$ (blue, **2**); (iii) tetrahedral $CoCl_2(L^c)_2$ (green, **3**). Redox-induced chemical reactions of these compounds then provide access to three further new cobalt derivatives of 2-(arylazo)pyridine. One-electron reduction of **3** by dilute aqueous hydrazine produced complex **4**, a distorted trigonal-bipyramidal $CoCl(L^c)_2$ complex isostructural with **2** in near-quantitative yield. This reaction is chemically reversible: oxidation of **4** with Cl_2 regenerates **3**, highlighting the

Received: July 13, 2013
Published: November 21, 2013

   dx.doi.org/10.1021/ic4018079 | *Inorg. Chem.* 2013, 52, 14040−14049

Chart 1

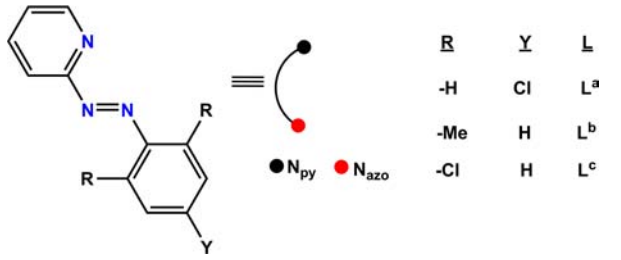

R	Y	L
-H	Cl	L^a
-Me	H	L^b
-Cl	H	L^c

Scheme 1[a]

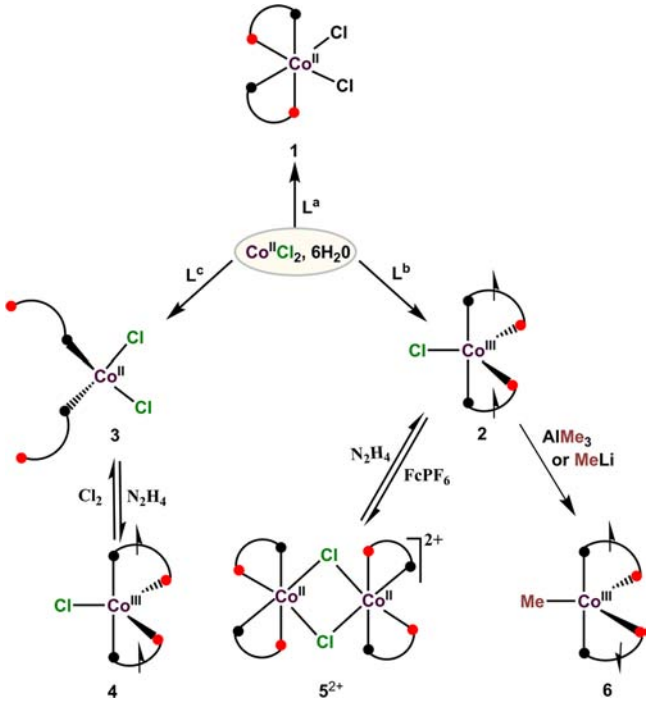

[a]The assignment of the oxidation states of the ligands and metal shown in the scheme is discussed in detail in the subsequent sections dealing with the electronic structure.

hemilabile[17] nature of azopyridine ligands. In contrast, oxidation of **2** with ferrocinium hexafluorophosphate ($FcPF_6$) produced a dichloro-bridged Co_2 complex of composition $[CoCl(L^b)_2]_2^{2+}$ ($\mathbf{5}^{2+}$). Oxidation of **2** is also reversible: reduction of $\mathbf{5}^{2+}$ with dilute aqueous hydrazine regenerates **2** in quantitative yield. Finally, we have also isolated a violet complex, $CoMe(L^c)_2$ (**6**), from the reaction of **2** with an equimolar quantity of $AlMe_3$. Complex **6** is a distorted trigonal bipyramid, similar in structure to both **2** and **4**. An identical product was also obtained from the reaction of **2** with an equimolar quantity of MeLi. Elemental analyses of all six complexes corroborate the formulations given above (see the Experimental Section).

Characterization: X-ray Crystallography, Magnetic Susceptibility, and Spectroscopy. All six complexes have been characterized using X-ray crystallography. Crystallographic details are given in Table 1, key bond lengths and angles in Table 2, and ORTEP plots in Figure 1.

Figure 1 shows that in the five complexes **1**, **2**, and **4**–**6** the azoaromatic ligands bind in the more common bidentate fashion, while in complex **3**, only the pyridine nitrogen, N_{py}, is coordinated. A similar monodentate coordination mode of 2-(arylazo)pyridine and for related ligands containing imidazole has been reported[18] in only a few instances. Complexes **1** and $\mathbf{5}^{2+}$ have approximate octahedral coordination about the cobalt center, while the monodentate coordination mode in **3** leads to an approximately tetrahedral arrangement. Complexes **2** and **4** have a five-coordinate, approximately trigonal-bipyramidal structure with a chloro ligand and two azo nitrogen atoms occupying the equatorial plane (Cl–Co–N_{azo} = 114° and Cl–Co–N_{py} = 93°). Complex **6** also adopts a five-coordinate structure, qualitatively similar to that of **2** and **4**, although the geometry is more distorted toward a square pyramid (Me–Co–N_{azo} = 110° and Me–Co–N_{py} = 89°) with the methyl group in the axial position.

The N–N distance in 2-(arylazo)pyridine ligands is commonly used as an indicator of the oxidation state of the coordinated group,[14a] and values of 1.24–1.27 Å in **1**, **3**, and $\mathbf{5}^{2+}$ are characteristic of neutral ligands. The N–N bond lengths in **2** and **4** lie in a narrow window between 1.313(3) and 1.317(2) Å, approximately 0.05 Å longer than those in **1**, **3**, and $\mathbf{5}^{2+}$, while those in **6** are even longer, at 1.330(5) and 1.337(5) Å.

The Co–N_{azo} lengths are also indicative of significant changes in the electronic structure in **2**, **4**, and **6** vs **1**, **3**, and $\mathbf{5}^{2+}$: while the Co–N_{azo} bonds in complexes **1**, **3**, and $\mathbf{5}^{2+}$ are appreciably *longer* than their Co–N_{py} counterparts (2.33 vs 2.12 Å), the opposite is true in **2**, **4**, and **6** (1.84 vs 1.90 Å). Subtle differences between **6** and **2**/**4** are also apparent in the N–N and Co–N_{azo} bond lengths, which are ~0.02 Å longer and shorter, respectively, in **6** compared to **2**/**4**. These changes in the Co–N distances indicate a transition from a neutral ligand in **1**, **3**, and $\mathbf{5}^{2+}$, where the azo group is a weak donor[19] compared to N_{py} to an anionic one in **2**, **4**, and **6**. The N–N stretching frequencies, ν(N–N), in the IR spectra reinforce this picture: values of 1430 cm^{-1} (**1** and **3**) and 1435 cm^{-1} ($\mathbf{5}^{2+}$) are very similar to 1440 cm^{-1} for free L^a and substantially greater than 1220 cm^{-1} in **2**. As a whole, the structural and IR data are consistent with an accumulation of negative charge[14e] on the azo groups that increases in the order (**1**, $\mathbf{5}^{2+}$) < (**2**, **4**) < **6**. The assignments of oxidation states will be discussed in detail in the section dealing with electronic structure calculations.

Magnetic susceptibility measurements for complexes **1**, **3**, and $\mathbf{5}[PF_6]_2$ were made on polycrystalline samples in the temperature range 2–300 K. The temperature dependencies of the magnetic behavior (μ_{eff} vs T plot; μ_{eff} = effective magnetic moment) are shown in Figure 2. The effective magnetic moments (μ_{eff}) of **1** and **3** are virtually temperature-independent from 50 to 300 K at 4.65 and 4.45 μ_B, respectively, and decrease rapidly at low temperature (<50 K). The magnetic moments of 4.65 and 4.45 μ_B for **1** and **3** are somewhat higher than the spin-only value (3.87 μ_B; $[4S(S+1)]^{1/2}$; $S = {}^3/_2$) anticipated for mononuclear high-spin Co^{II}. In the case of octahedral **1**, this may be a consequence of some residual first-order orbital angular momentum in the T ground state, while in tetrahedral **3**, it may be due to second-order mixing of the T excited state into the A ground state. A similarly higher magnetic moment (4.51 μ_B) for tetrahedral $CoCl_2(py)_2$ (py = pyridine) was rationalized in these terms.[20] The value of 5.84 μ_B for $\mathbf{5}^{2+}$ is characteristic[21] of a weakly interacting bimetallic high-spin Co^{II} species. The magnetic moment remains almost unaltered in the temperature range 300–100 K, and at much lower temperatures (<100 K), the magnetic moment decreases rapidly because of the intermolecular antiferromagnetic interaction.

dx.doi.org/10.1021/ic4018079 | Inorg. Chem. 2013, 52, 14040–14049

Table 1. Crystallographic Data for Complexes 1−6

	1	2	3	4	$5[PF_6]_2\cdot 2CH_2Cl_2$	6
empirical formula	$C_{22}H_{16}N_6CoCl_4$	$C_{26}H_{26}N_6CoCl$	$C_{22}H_{14}N_6CoCl_6$	$C_{22}H_{14}Cl_5N_6Co$	$C_{54}H_{56}N_{12}P_2F_{12}Co_2Cl_4$	$C_{27}H_{29}N_6Co$
mol mass	565.14	516.91	634.02	598.57	1493.61	496.49
temp (K)	293	150	293	293	293	293
cryst syst	monoclinic	monoclinic	monoclinic	orthorhombic	monoclinic	orthorhombic
space group	$P2_1/c$	$P2_1/c$	$C2/c$	$Pbca$	$P2_1/n$	$pbc2_1$
a (Å)	7.6267(4)	19.276(2)	13.346(5)	14.090(5)	13.244(7)	8.0200(6)
b (Å)	22.0463(12)	8.5130(11)	13.800(5)	14.745(5)	21.071(10)	16.8828(13)
c (Å)	13.9760(8)	16.017(2)	14.367(5)	23.495(5)	23.312(12)	37.398(3)
α (deg)	90	90	90	90	90	90
β (deg)	103.286(1)	109.519(3)	105.227(5)	90	93.632(15)	90
γ (deg)	90	90	90	90	90	90
V (Å^3)	2287.0(2)	2477.3(5)	2553.1(16)	4881(3)	6493(6)	5063.7(7)
Z	4	4	4	8	4	8
D_{calcd} (g cm^{-3})	1.641	1.386	1.650	1.629	1.528	1.303
cryst dimens (mm)	0.11 × 0.15 × 0.18	0.11 × 0.17 × 0.22	0.10 × 0.18 × 0.20	0.12 × 0.15 × 0.19	0.15 × 0.18 × 0.21	0.09 × 0.12 × 0.17
θ range (deg)	1.8−24.6	1.1−25.9	2.2−25.3	1.7−27.8	1.3−25.0	1.1−23.3
GOF	0.70	0.74	1.03	1.03	0.95	0.85
reflns collected	20431	23796	11960	51895	72836	35522
unique reflns	3842	4825	2330	5733	11224	7305
final R indices [$I > 2\sigma(I)$]	R1 = 0.0299, wR2 = 0.0863	R1 = 0.0374, wR2 = 0.1209	R1 = 0.0421, wR2 = 0.1172	R1 = 0.0330, wR2 = 0.0825	R1 = 0.0605, wR2 = 0.1911	R1 = 0.0389, wR2 = 0.1308

Table 2. Selected Experimental Bond Distances (Å) and Bond Angles (deg) for Complexes 1, 2, 4, and 6

	1 (X = Cl1, Cl2)	2 (X = Cl)	4 (X = Cl)	6 (X = Me)
		Bond Distances (Å)		
Co1−X	2.3533(8), 2.3435(8)	2.2815(7)	2.2892(10)	2.014(7)
Co1−N1	2.150(2)	1.9026(19)	1.9075(18)	1.886(4)
Co1−N3	2.368(2)	1.842(2)	1.8512(18)	1.835(4)
Co1−N4	2.080(2)	1.8957(19)	1.9085(18)	1.884(3)
Co1−N6	2.296(2)	1.845(2)	1.8481(17)	1.841(4)
N2−N3	1.262(3)	1.313(3)	1.315(2)	1.330(5)
N5−N6	1.260(3)	1.314(3)	1.317(2)	1.337(5)
		Bond Angles (deg)		
N1−Co1−N3	70.62(8)	80.11(9)	79.86(7)	80.77(16)
N4−Co1−N6	72.23(8)	80.17(9)	79.88(7)	81.01(16)
N1−Co1−X	94.30(6), 90.26(7)	95.21(6)	91.74(5)	90.92(19)
N3−Co1−X	164.10(6), 81.74(6)	115.47(7)	112.72(6)	113.0(2)
N4−Co1−X	93.27(6), 160.03(7)	91.22(6)	93.48(5)	87.89(19)
N6−Co1−X	84.85(6), 99.02(6)	112.92(7)	117.40(5)	108.9(2)

In contrast to **1**, **3**, and $\mathbf{5}^{2+}$, complexes **2**, **4**, and **6** are all diamagnetic and display highly resolved ^{1}H NMR spectra. A representative spectrum, that of **2** in dimethyl sulfoxide (DMSO-d_6), is shown in Figure 3, and spectra of **4** and **6** are given as Supporting Information (SI; Figures S1 and S2). In Figure 3, all seven aromatic proton resonances for one ligand are visible in the range δ 8.2−6.8 ppm. The aromatic resonances for **4** appear in a similar region, but those for **6** are shifted to higher fields (SI, Figures S1 and S2). The two methyl resonances of **2** appear at δ 2.34 and 0.94 ppm, confirming that the two ligands are magnetically equivalent. Complexes **2**, **4**, and **6** are intensely colored and absorbed strongly in the low-energy visible range, 630−680 nm (Figure 4). The major transitions (ε > 7000 M^{-1} cm^{-1}) in **2** and **4** are also associated with ill-defined shoulders at ca. 740 and 910 nm, which are assigned as d−d transitions (Gaussian fits of the UV−vis spectra of complexes **2** and **4** are given as SI, Figures S3 and S4).

Cyclic Voltammetry. The redox behavior of complexes **1**−**6** was studied by cyclic voltammetry and related electrochemical techniques; the data are collected in Table 3. Complex **1** showed two reductions in CH_2Cl_2 using tetrabutylammonium perchlorate (TBAP) as the supporting electrolyte at −0.38 and −0.63 V along with a quasi-reversible oxidation at 0.78 V with ΔE_p, 110 mV (SI, Figure S5). While the reductions are ligand-centered,[14a] the oxidative response is due to a Co^{II}/Co^{III} couple. For comparison, the Co^{II}/Co^{III} couple in $[Co(pap)_3]^{2+}$ [pap = 2-(phenylazo)pyridine] appears[22] at 1.09 V. Voltammetric measurements of complexes **2**−**6** were made in acetonitrile using tetraethylammonium perchlorate as the supporting electrolyte. Voltammograms of complex **2** at multiple scan rates are displayed in Figure 5, revealing two reversible responses at 0.39 and −0.77 V. A differential pulse voltammogram and i_p versus $v^{1/2}$ plots for both couples are given in the SI, Figures S6−S8. The peak-to-peak separation (ΔE_p) for the response at positive potential is 80−90 mV, comparable to that of the Fc/Fc$^+$ (Fc$^+$ = ferrocenium ion)

dx.doi.org/10.1021/ic4018079 | Inorg. Chem. 2013, 52, 14040−14049

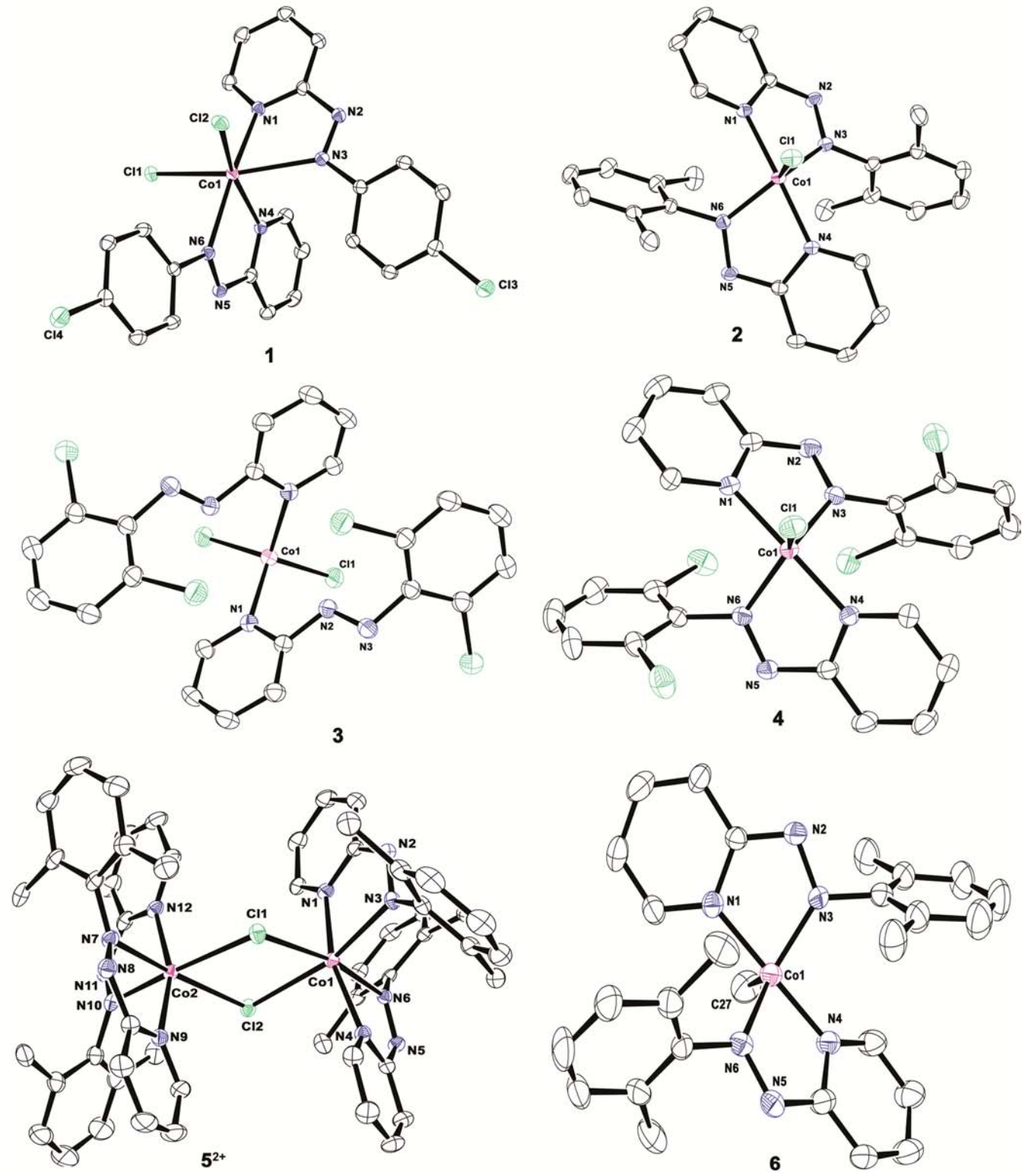

Figure 1. ORTEP diagrams of complexes **1**−**6**. Complexes **1**−**4** and **6** are neutral, while complex $\mathbf{5}^{2+}$ is dicationic. The counteranions ($[PF_6]^-$), two solvent molecules (CH_2Cl_2) in $\mathbf{5}[PF_6]_2\cdot 2CH_2Cl_2$, and all hydrogen atoms of the complexes are omitted for clarity.

couple under the same experimental conditions (80 mV). Moreover, the cathodic current height (i_{pc}) for the reduction couple (at −0.77 V) is ∼2.8 times larger than that of the oxidative couple and, furthermore, ΔE_p is 50−55 mV. All of these together establish that it is a single-step, two-electron-transfer process. Exhaustive electrolysis experiments failed and resulted in a continuous current. These observations are not unexpected because this complex undergoes chemical changes upon both oxidation and reduction: oxidation of **2** produces complex $\mathbf{5}^{2+}$ (vide supra), and reduction results in decomposition. Tetrahedral complex **3** displayed a single reversible wave at −0.62 V with a current height comparable to that of the Fc/Fc^+ couple, indicating a one-electron process (SI, Figure S9). This complex, however, undergoes a chemical trans-

dx.doi.org/10.1021/ic4018079 | *Inorg. Chem.* 2013, 52, 14040−14049

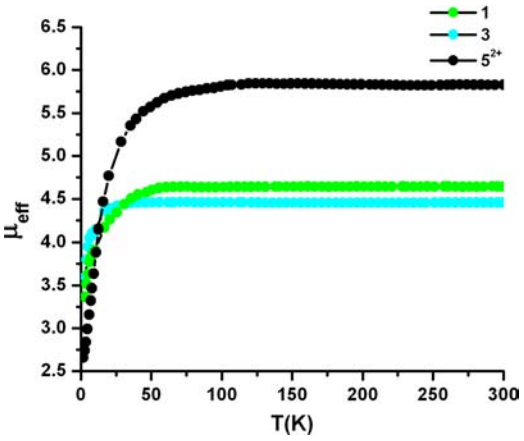

Figure 2. SQUID magnetic data of complexes **1**, **3**, and $\mathbf{5}[PF_6]_2$.

formation upon reduction at 300 K, producing complex **4** (vide supra). The nature of the cyclic voltammogram for complex **4** is very similar to that of **2**, although the reductive response is irreversible (SI, Figure S10). The Co_2^{II} complex $\mathbf{5}^{2+}$ shows two oxidative waves at 0.48 and 1.22 V, although the second wave is not well resolved, indicating chemical degradation. The separation between the two waves is comparable to that in other Cl_2-bridged Ru_2 complexes.[23] An irreversible reductive response with a somewhat higher current height was also noted near −0.81 V (SI, Figure S11): we have already noted that chemical reduction of complex $\mathbf{5}^{2+}$ produces **2** in a near-quantitative yield. Successive oxidation processes in the latter complex are ascribed to Co^{II}/Co^{III} responses, and the Co−Me complex **6** also showed two responses at +0.46 and −1.26 V with similar current height (SI, Figure S12): the response at positive potential is assigned as oxidation of the coordinated azoanion ligand, and it occurs at a potential comparable to that in the other two five-coordinate diradical complexes, **2** and **4**. Thus, the cyclic voltammetric responses of the complexes are consistent with the choices of chemical oxidant and reductant used to achieve the bulk syntheses described previously.

Electronic Structure Analysis. The optimized structures of various spin states of the monometallic complexes **1**−**4** and **6** are summarized in Table 4, along with Mulliken spin densities and values of $\langle S^2 \rangle$. In the case of both **1** and **3**, the most stable state is a quartet, consistent with the magnetic data, and the

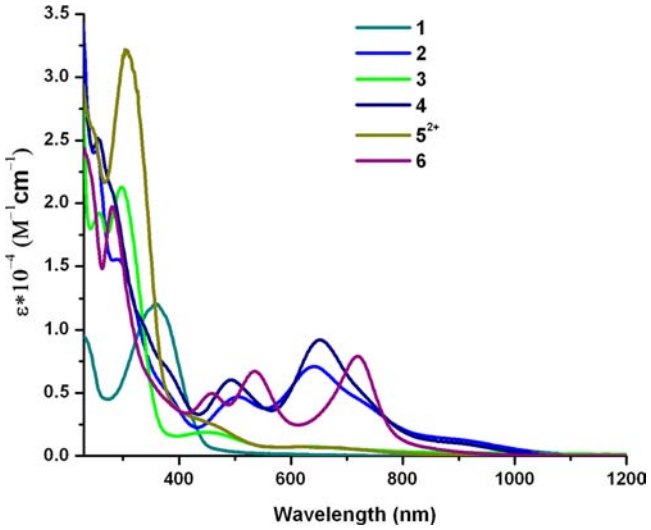

Figure 4. Electronic spectra of complexes **1**−**6** in acetonitrile.

Table 3. Cyclic Voltammetric[a] and UV−Vis Spectral Data[e] of Complexes 1−6

complex	cyclic voltammetric data:[a] $E_{1/2}$,[b] V (ΔE_p, mV)	UV−vis spectral data:[e] λ_{max}[e] (ε, 10^4 M^{-1} cm^{-1})
1	0.78[c] (110), −0.38[c] (120), −0.63 (80)	360 (1.2)
2	0.39 (85), −0.77 (50)	910,[f] 740,[f] 640 (0.7), 500 (0.47), 290[f]
3	−0.62 (90)	454,[f] 300 (2.1), 260 (1.9)
4	0.65 (85), −0.59[d]	910,[f] 730,[f] 650 (0.92), 490 (0.6), 260[f]
$\mathbf{5}^{2+}$	0.48 (80), 1.22,[d] −0.81[d]	460,[f] 360 (1.2)
6	0.46 (110), −1.26 (95)	720 (0.78), 535 (0.67), 460 (0.5), 280 (1.95), 230 (2.4)

[a]Dichloromethane solution for complex **1** (supporting electrolyte Bu_4NClO_4); acetonitrile solution for complexes **2**−**6** (supporting electrolyte Et_4NClO_4), working electrode platinum, reference electrode Ag/AgCl. [b]$E_{1/2} = 0.5(E_{pa} + E_{pc})$, where E_{pa} and E_{pc} are anodic and cathodic peak potentials, respectively, $\Delta E_p = E_{pa} - E_{pc}$, and scan rate 50 mV s^{-1}. [c]Quasi-revesible. [d]Irreversible. [e]Wavelength in nanometers; molar extinction coefficients in M^{-1} cm^{-1} in an acetonitrile solvent. [f]Shoulder.

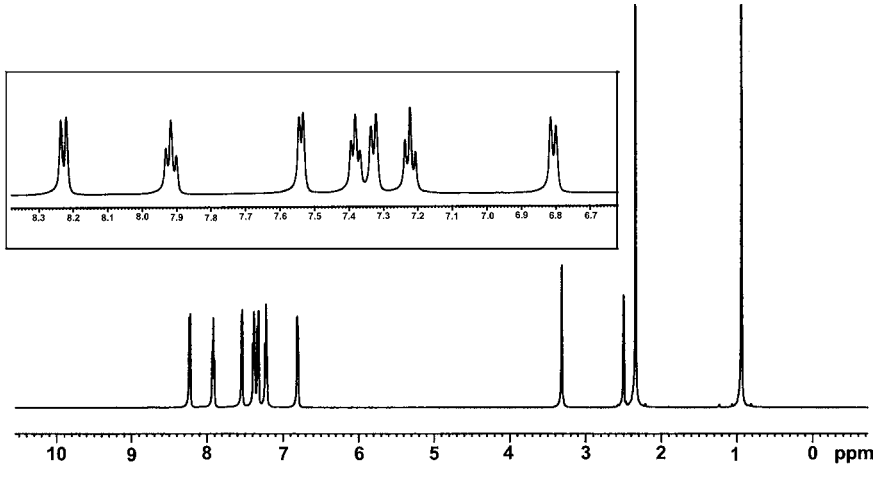

Figure 3. ^1H NMR spectrum of complex **2** in DMSO-d_6. Inset: aromatic proton resonances.

dx.doi.org/10.1021/ic4018079 | Inorg. Chem. 2013, 52, 14040−14049

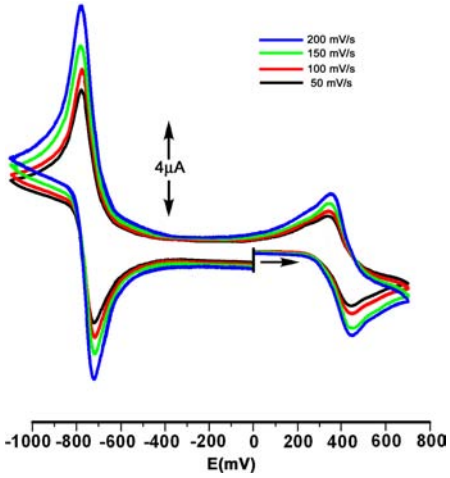

Figure 5. Cyclic voltammograms of complex **2** at different scan rates in an acetonitrile solvent.

optimized bond lengths are similar to those measured by X-ray diffraction. In particular, the optimized N═N bond lengths are short (1.25 Å), and in the case of **1**, the Co−N_{azo} bond is longer than Co−N_{py}. The spin densities of ∼2.70 on the metal centers are strongly indicative of a high-spin Co^{II} configuration, while those on the ligands [ρ(L) < 0.1] suggest a neutral formulation. Computational analysis is therefore unequivocal in supporting a Co^{II} oxidation state for **1** and **3**.

Turning to complexes **2**, **4**, and **6**, the electronic structure landscape is rather more complex. The diamagnetism of all three complexes is, in principle, consistent with a range of formulations including (i) low-spin Co^{III} (S_{Co} = 0) with two antiferromagnetically coupled ligand radicals ($S_L = \pm^1/_2$) (ii) intermediate-spin Co^{III} (S_{Co} = 1) coupled antiferromagnetically to two ligand radicals ($S_L = +^1/_2$), or (iii) low-spin Co^{II} ($S_{Co} = {}^1/_2$) coupled antiferromagnetically to a single unpaired electron, either localized on a single ligand or delocalized over both. The ground-state electronic structures of complexes **2** and **4** are very similar, and the spin densities and magnetic orbitals shown in Figure 6 are typical of scenario (ii) identified above. In both cases, the ground state is a BS(2,2) broken-symmetry singlet with substantial spin contamination ($\langle S^2\rangle$ = 1.01) and opposing Mulliken spin populations on the cobalt (1.21) and ligand (−0.65 per L). The overlaps between corresponding orbitals shown in Figure 6 clearly indicate the presence of *two* singly occupied orbitals on the metal, d_{xy} and $d_{x^2-y^2}$, which lie in the equatorial plane of the trigonal bipyramid and overlap with the singly occupied in-phase and out-of-phase linear combinations of the azo π^* orbitals. This overlap reduces the spin density at cobalt from an idealized value of 2.0 for a local triplet configuration. An alternative interpretation of the Mulliken spin density of 1.21 at cobalt is a low-spin Co^{II} species (scenario (iii) above). However, the presence of a net spin density >1.0 and *two* approximately singly occupied d orbitals is more consistent with the intermediate-spin Co^{III} description. The L_2 unit is therefore effectively reduced by two electrons, driving the substantial elongation of the N═N distances relative to those in **1** and **3** (1.31 vs 1.24 Å).

While the gross structure of **6** is superficially rather similar to those of **2** and **4**, the electronic structure is significantly different. The ground state (Figure 7) is again a broken-symmetry singlet, but the absence of significant spin density on the cobalt center, combined with opposing spin densities on the ligand [ρ(L) = ± 0.65], is indicative of scenario (i) with a low-spin Co^{III} center in conjunction with a doubly reduced (L_2) manifold [BS(1,1)]. The contrast between **2** and **4**, on the one hand, and **6**, on the other hand, is caused by the strongly σ-donating methyl group, which introduces a substantial splitting within the $d_{xy}/d_{x^2-y^2}$ pair and so favors a low-spin Co^{III} configuration with a more square-pyramidal geometry (optimized Me−Co−N_{azo} = 107° vs Cl−Co−N_{azo} = 113° in **2**). The very short Co−Me bond in **6** is also a direct consequence of the low-spin configuration and its preference for a square-pyramidal coordination geometry. We note here that the contrast between **2**/**4** and **6** is very similar to that identified by Wieghardt and co-workers in a Co(diimine)$_2$Me complex,[24] where it proved possible to converge on both electronic structure scenarios (i) and (ii) identified above (separated by 1 kcal mol^{-1}) in a single complex. The more stable of the two, the BS(1,1) solution, is identical with our description of **6**, while BS(2,2) corresponds to our description of **2** and **4**. In no case in this study did we converge on scenario (iii) noted above, with a low-spin Co^{II} complex and a single unpaired spin delocalized over the ligands, although such a case was identified in Wieghardt's iodide analogue,[24a] Co(diimine)$_2$I.

CONCLUSION

The chemical reactions described in this paper have revealed some unusual aspects of the coordination and redox chemistry of Co^{II} and Co^{III} complexes of 2-(arylazo)pyridines. While complex **1** adopts six-coordination commonly observed for closely related ligands, an increase in steric bulk (ligands L^b and L^c) results in lower coordination numbers of 5 (complexes **2**, **4**, and **6**) or 4 (complex **3**). Complexes **1**, **3**, and **5** feature high-

Table 4. Optimized Structural Parameters and Mulliken Spin Populations for 1−4 and 6

	1	3	2		4		6	
	$S = {}^3/_2$	$S = {}^3/_2$	S = 0	S = 1	S = 0	S = 1	S = 0	S = 1
Co−N_{py}	2.17,[b] 2.18[a]	2.11	1.94	1.94	1.93	1.93	1.94	1.96
Co−N_{azo}	2.39,[b] 2.49[a]	3.05	1.91	1.99	1.98	1.99	1.91	1.95
Co−X	2.34,[c] 2.35[d]	2.27	2.31	2.26	2.28	2.25	2.00	1.97
N═N	1.25, 1.26	1.24	1.31	1.30	1.31	1.30	1.32	1.32
$\langle S^2\rangle$	3.76	3.76	1.01	2.05	1.14	2.06	0.58	2.04
ρ(Co)	2.70	2.72	1.21	0.83	1.28	0.81	0.03	0.35
ρ(X)	0.09	0.11	0.10	0.00	0.10	0.00	−0.01	0.00
ρ(L)	0.12	0.03	−0.65	0.58	−0.60	0.60	±0.63	0.82
relative energy/eV	0.0	0.0	0.0	0.20	0.0	0.16	0.0	0.36

[a]Axial. [b]Equatorial. [c]Trans to pyridine. [d]Trans to azo.

dx.doi.org/10.1021/ic4018079 | Inorg. Chem. 2013, 52, 14040−14049

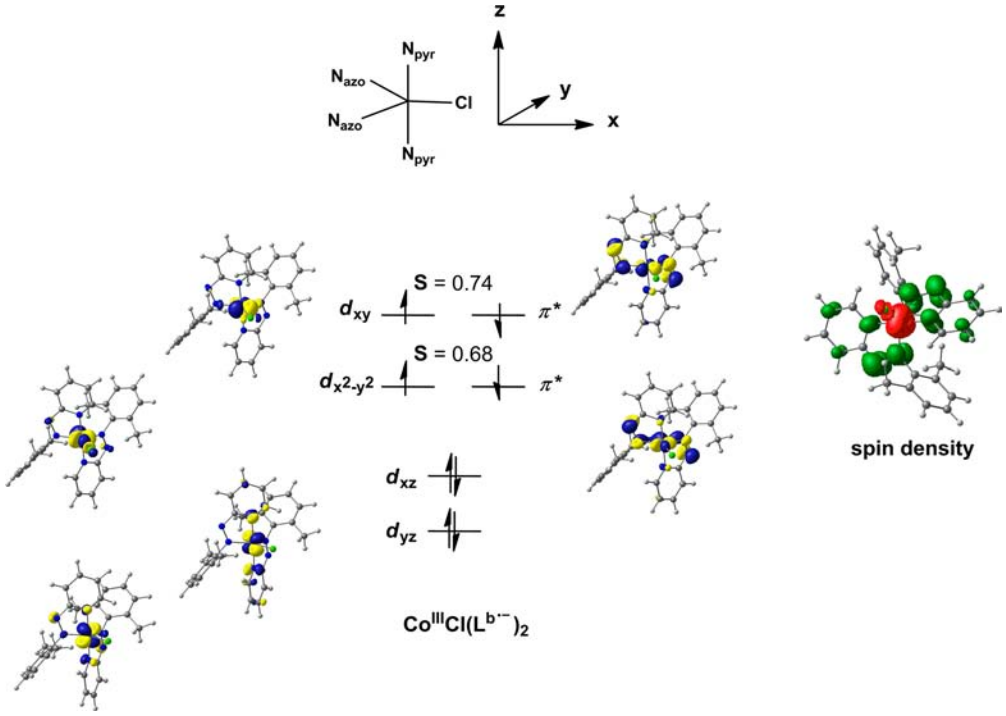

Figure 6. Magnetic orbitals and net spin densities for the BS(2,2) ground state of $CoCl(L^{b\bullet-})_2$ (**2**).

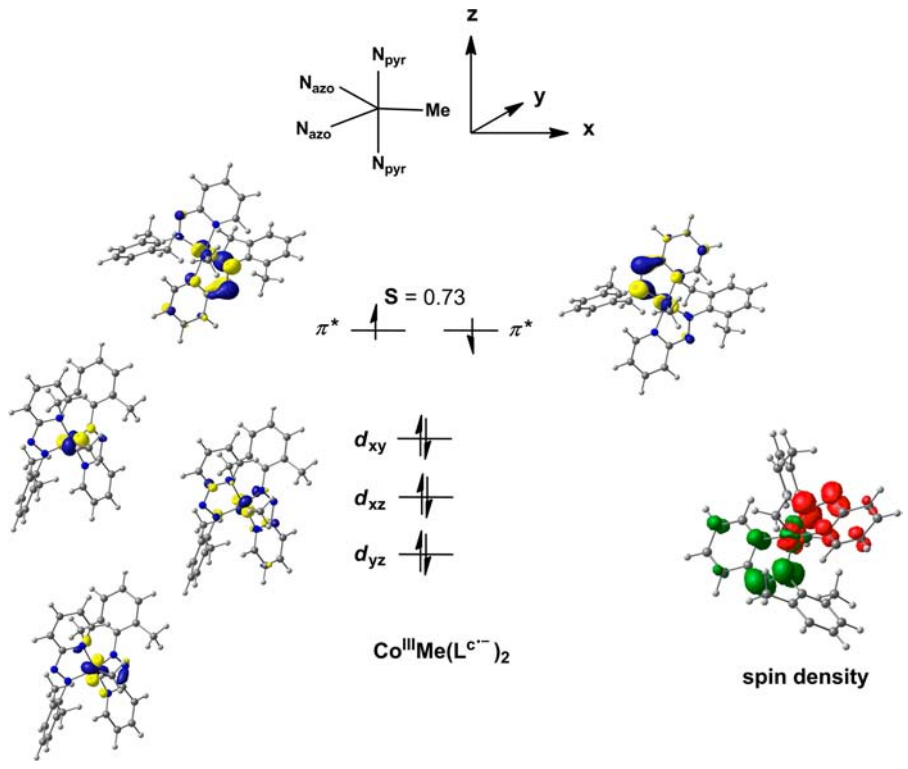

Figure 7. Magnetic orbitals and net spin densities for the BS(1,1) ground state of $CoMe(L^{c\bullet-})_2$ (**6**).

spin Co^{II} centers, while five-coordinate **2** and **4** have Co^{III} in an unusual intermediate $S = 1$ spin state in combination with two singly reduced azoaromatic ligand radicals. The reversible formation of **4** by *reduction* of **3** is particularly interesting because the metal center is *oxidized* from Co^{II} to Co^{III}, while both azo ligands are reduced by one electron. Conversely, the oxidation of **2** to $\mathbf{5}^{2+}$ induces *reduction* at the metal centers, with both ligands being oxidized to the neutral form. The chemical transformations **2** ↔ $\mathbf{5}^{2+}$ and **3** ↔ **4** therefore involve redox-induced electron transfer[25] (RIET): changing the oxidation level of one of the two ligands induces a further internal electron transfer between the metal and the other ligand. A similar RIET was reported[26] previously by Wieghardt et al. in a manganese complex of 2,6-diiminopyridine ligand (L^2), where a high-spin Mn^{II} complex $[Mn^{II}(L^2)_2]^{2+}$ ($S = {}^5/_2$) underwent reversible one-electron reduction to generate diamagnetic

dx.doi.org/10.1021/ic4018079 | *Inorg. Chem.* 2013, 52, 14040−14049

$[Mn^{III}\{(L^2)^{\bullet-}\}_2]^+$ (S = 0). The impact of the ligand environment on the Co^{III} center is illustrated by complex **6**, which is closely related to **2** and **4** (in so much as the ligands are singly reduced), but the strong σ-donor methyl ligand stabilizes a low-spin (S = 0) configuration at Co^{III}. The 2-(arylazo)pyridine ligands in the reduced state therefore stabilize Co^{III} in either low (**6**) or intermediate (**2** and **4**) spin states (S = 0 or 1), while the corresponding oxidized ligands stabilize high-spin states of Co^{II} (**1**, **3**, and $\mathbf{5}^{2+}$).

EXPERIMENTAL SECTION

Materials. All of the reagents and chemicals were purchased from commercial sources and used without further purification. TBAP was prepared and recrystallized as reported earlier.[27] ***Caution!*** *Perchlorates have to be handled with care and appropriate safety precautions!*

Physical Measurements. UV−vis absorption spectra were recorded on a Perkin-Elmer Lambda 950 UV−vis spectrophotometer and a J&M TIDAS instrument. Variable-temperature (2−300 K) magnetization data were recorded in a 0.1 T magnetic field on a SQUID magnetometer (MPMS Quantum Design). IR spectra were obtained using a Perkin-Elmer 783 spectrophotometer. ^{1}H NMR spectra were recorded on a Bruker Avance 300 or 500 MHz spectrometer, and $SiMe_4$ was used as the internal standard. A Perkin-Elmer 240C elemental analyzer was used to collect microanalytical data (C, H, and N). Electrospray ionization mass spectrometry (ESI-MS) spectra were recorded on a micromass Q-TOF mass spectrometer (serial no. YA 263). Cyclic voltammetry potentials were measured under a nitrogen atmosphere using a Ag/AgCl reference electrode, with a platinum disk working electrode and a platinum wire auxiliary electrode, in acetonitrile or dichloromethane containing 0.1 M Et_4NClO_4 or 0.1 M Bu_4NClO_4, respectively. A platinum wire gauge working electrode was used for exhaustive electrolyses. The $E_{1/2}$ value for the ferrocenium/ferrocene couple under our experimental conditions was 0.4 V.

Synthesis. All of the ligands L^{a-c} were synthesized following a literature procedure[28] previously reported for L^a. The disubstituted nitrosoarenes were synthesized by following a reported synthetic method.[29] The ligands $L^{b,c}$ are new, and their yields and characterization data are as follows:

L^b. Yield: 20%. IR (KBr, cm^{-1}): 1579 [ν(C═N) + ν(C═C)], 1425 [ν(N═N)]. Anal. Calcd for $C_{13}H_{13}N_3$: C, 73.91; H, 6.20; N, 19.89. Found: C, 73.90; H, 6.19; N, 19.88. ESI-MS: m/z 234 ([M + Na]$^+$). ^{1}H NMR (500 Mz): δ 8.76 (d, 1H, J = 4.5 Hz), 7.89 (t, 1H, J = 7.5 Hz), 7.72 (d, 1H, J = 8 Hz), 7.42 (t, 1H, J = 6.5 Hz), 7.22−7.19 (m, 1H), 7.15 (d, 2H, J = 7.5 Hz), 2.47 (s, 6H).

L^c. Yield: 60%. IR (KBr, cm^{-1}): 1580 [ν(C═N) + ν(C═C)], 1433 [ν(N═N)]. Anal. Calcd for $C_{11}H_7N_3Cl_2$: C, 52.41; H, 2.80; N, 16.67. Found: C, 52.39; H, 2.79; N, 16.65. ESI-MS: m/z 275 ([M + Na]$^+$).^{1}H NMR (500 Mz): δ 8.73 (d, 1H, J = 4 Hz), 7.89 (t, 1H, J = 7.5 Hz), 7.78 (d, 1H, J = 8 Hz), 7.43 (t, 1H, J = 6 Hz), 7.37 (d, 2H, J = 8.5 Hz), 7.16 (m, 1H).

*Preparation of $Co(L^a)_2Cl_2$ (**1**).* A mixture of 240 mg (1.01 mmol) of $CoCl_2$, $6H_2O$, and 440 mg (2.02 mmol) of L^a in 50 mL methanol was refluxed for 4 h. The resulting brown solution was evaporated to dryness. The crude residue was subsequently extracted with dichloromethane and recrystallized from a dichloromethane−hexane solution. Yield: 91% (515 mg). IR (KBr, cm^{-1}): 1580 [ν(C═N) + ν(C═C)], 1430 [ν(N═N)]. Anal. Calcd for $C_{22}H_{16}N_6CoCl_4$: C, 46.76; H, 2.85; N, 14.87. Found: C, 46.75; H, 2.84; N, 14.86.

Complexes **2** and **3** were prepared following a synthesis procedure identical with that described above and using the appropriate ligands: L^b for complex **2** and L^c for complex **3**. Their yield and characterization data are as follows:

*$Co(L^b)_2Cl$ (**2**).* Color: blue. Yield: 80% (413 mg). IR (KBr, cm^{-1}): 1599 [ν(C═N) + ν(C═C)], 1220 [ν(N═N)]. Anal. Calcd for $C_{26}H_{26}N_6CoCl$: C, 60.41; H, 5.07; N, 16.26. Found: C, 60.39; H, 5.05; N, 16.25. ESI-MS: m/z 481 ([M − Cl]$^+$). ^{1}H NMR (500 Mz): δ 8.22 (d, 1H, J = 8.0 Hz), 7.91 (t, 1H, J = 7.5 Hz), 7.53 (d, 1H, J = 6 Hz), 7.38 (t, 1H, J = 6.5 Hz), 7.32 (d, 1H, J = 7 Hz), 7.22 (t, 1H, J = 7.5 Hz), 6.8 (d, 1H, J = 7.5 Hz), 2.34 (s, 3H), 0.94 (s, 3H).

*$Co(L^c)_2Cl_2$ (**3**).* Color: green. Yield: 90% (570 mg). IR (KBr, cm^{-1}): 1595 [ν(C═N) + ν(C═C)], 1435 [ν(N═N)]. Anal. Calcd for $C_{22}H_{14}N_6CoCl_6$: C, 41.68; H, 2.23; N, 13.25. Found: C, 41.67; H, 2.21; N, 13.24.

*Preparation of $Co(L^c)_2Cl$ (**4**).* To a methanolic (50 mL) solution of complex **3** (640 mg, 1 mmol) was added dropwise a methanolic solution of hydrazine hydrate with continuous stirring of the mixture. The solution became blue almost instantaneously, and the crude product was crystallized by the slow diffusion of a dichloromethane solution of the complex into hexane. Yield: 90% (540 mg). IR (KBr, cm^{-1}): 1597 [ν(C═N) + ν(C═C)], 1230 [ν(N═N)]. ESI-MS: m/z 563 ([M − Cl]$^+$). Anal. Calcd for $C_{22}H_{14}Cl_5N_6Co$: C, 44.14; H, 2.36; N, 14.04. Found C, 44.12; H, 2.35; N, 14.02. ^{1}H NMR (500 Mz): δ 8.36 (d, 1H, J = 8 Hz), 7.98 (t, 1H, J = 8 Hz), 7.78 (d, 1H, J = 8 Hz), 7.73 (d, 1H, J = 6 Hz), 7.58 (t, 1H, J = 6.5 Hz), 7.45 (t, 1H, J = 8.5 Hz), 7.2 (d, 1H, J = 8 Hz).

Preparation of $[Co(L^b)_2Cl]_2[PF_6]_2$ ($\mathbf{5}[PF_6]_2$). To an acetonitrile solution (60 mL) of complex **2** (100 mg, 0.19 mmol) was added 70 mg (0.21 mmol) of $FcPF_6$. The mixture was stirred for 2 h, and the color of the solution became brown. It was then evaporated under reduced pressure, and the crude mass was extracted with dichloromethane and crystallized from a dichloromethane−hexane solution. Yield: 80% (105 mg). IR (KBr, cm^{-1}): 1604 [ν(C═N) + ν(C═C)], 1435 [ν(N═N)]. Anal. Calcd for $C_{52}H_{52}N_{12}P_2F_{12}Co_2Cl_2$: C, 47.18; H, 3.96; N, 12.70. Found: C, 47.16; H, 3.95; N, 12.68.

*Preparation of $[Co(L^b)_2Me]$ (**6**).* To a dry tetrahydrofuran (THF) solution (50 mL) of complex **2** (50 mg, 0.1 mmol) was added in an inert atmosphere 65 μL of 1.6 M MeLi in THF. The solution became violet instantaneously, and the solution was evaporated to dryness. The crude residue was subsequently extracted with dichloromethane and recrystallized from a dichloromethane−hexane solution.

Yield: 80% (40 mg). IR (KBr, cm^{-1}): 1602 [ν(C═N) + ν(C═C)], 1210 [ν(N═N)]. ESI-MS: m/z 496 ([M]$^+$). Anal. Calcd for $C_{27}H_{29}N_6Co$: C, 65.32; H, 5.89; N, 16.93. Found: C, 65.31; H, 5.86; N, 16.91. ^{1}H NMR (500 Mz): δ 7.82 (d, 2H, J = 8.5 Hz), 7.55 (t, 2H, J = 8 Hz), 7.35 (d, 2H, J = 6 Hz), 7.28 (d, 2H, J = 7.5 Hz), 7.19 (t, 4H, J = 7.5 Hz), 2.03 (6H), 1.19 (6H), 0.8 (3H).

X-ray Crystallography. Crystallographic data for complexes **1**−**4**, $\mathbf{5}[PF_6]_2$, and **6** are collected in Table 1. Suitable X-ray-quality crystals of these complexes are obtained by either the slow evaporation of a dichloromethane−hexane solution of the complex or the slow diffusion of a dichloromethane solution of the complex into hexane. All data were collected on a Bruker SMART APEX-II diffractometer, equipped with graphite-monochromated Mo Kα radiation (λ = 0.71073 Å) and were corrected for Lorentz polarization effects. **1**: A total of 20431 reflections were collected, of which 3842 were unique (R_{int} = 0.048), satisfying the $I > 2\sigma(I)$ criterion, and were used in subsequent analysis. **2**: A total of 23796 reflections were collected, of which 4825 were unique (R_{int} = 0.052). **3**: A total of 11960 reflections were collected, of which 2330 were unique (R_{int} = 0.064). **4**: A total of 51895 reflections were collected, of which 5733 were unique (R_{int} = 0.049). $\mathbf{5}[PF_6]_2\cdot 2CH_2Cl_2$: A total of 72836 reflections were collected, of which 11379 were unique (R_{int} = 0.063). **6**: A total of 35522 reflections were collected, of which 7305 were unique (R_{int} = 0.033). The structures were solved by employing the *SHELXS-97* program package[30a] and were refined by full-matrix least squares based on F^2 (*SHELXL-97*).[30b] All hydrogen atoms were added in calculated positions.

Computational Methods. All DFT calculations presented in this paper were carried out using the *Gaussian 09* program package.[31] Geometry optimizations were performed without imposing geometric constraints (C_1 symmetry), and stationary points were subsequently confirmed to be minima by vibrational analysis (no imaginary frequencies). All calculations utilized the B3LYP hybrid functional.[32] The ability of modern DFT to accurately predict the position of spin-state equilibria has been debated extensively in recent years. While it is clear that the separation between the two spin isomers is highly dependent on the chosen functional, the majority of functionals appear

dx.doi.org/10.1021/ic4018079 | Inorg. Chem. 2013, 52, 14040−14049

to reproduce important trends with encouraging accuracy. The TZVP basis set[33] of triple-ζ quality with one set of polarization functions was used on cobalt, on all atoms directly bonded to it (chlorine, nitrogen, and carbon), and on all other noncoordinated nitrogen atoms. For all other atoms (carbon, hydrogen, and chlorine substituents on the aromatic rings), polarized split-valence (SVP) basis sets[34] were used. The broken-symmetry approach first proposed by Ginsberg[35] and Noodleman and co-workers[36] has been employed for all complexes. A range of spin-polarized initial densities was tried in each case [BS(2,2), BS(1,1), etc.], but in all cases, different guesses (with the same total multiplicity) converged to the same minimum. Mulliken spin densities were used for analysis of the spin populations on the ligand and metal centers.[37]

■ ASSOCIATED CONTENT

Supporting Information

Relevant figures as noted in the text and X-ray crystallographic file in CIF format for **1**−**6**. This material is available free of charge via the Internet at http://pubs.acs.org.

■ AUTHOR INFORMATION

Corresponding Authors

*E-mail: john.mcgrady@chem.ox.ac.uk (DFT studies).
*E-mail: icsg@iacs.res.in.

Notes

The authors declare no competing financial interest.

■ ACKNOWLEDGMENTS

Financial support received from the Department of Science and Technology (Project SR/S1/IC/0031/2010), New Delhi, India, is gratefully acknowledged. S.G. sincerely thanks DST for a J. C. Bose fellowship. Crystallography for complexes **1**−**5**$^{2+}$ was performed at the DST-funded National Single Crystal Diffractometer Facility at the Department of Inorganic Chemistry, IACS. Single-crystal X-ray diffraction data of complex **6** were collected at the DBT-funded CEIB program (Project BT/01/CEIB/11/V/13) awarded to Department of Organic Chemistry, IACS, Kolkata, India. P.G. and S.K.R. are thankful to the Council of Scientific and Industrial Research for their fellowships.

Dedicated to Professor Karl Wieghardt for his pioneering contributions in the *Chemistry of Redox Noninnocent Ligands*.

■ REFERENCES

(1) Jørgensen, C. K. *Coord. Chem. Rev.* **1966**, *1*, 164−178.
(2) Butin, K. P.; Beloglazkina, E. K.; Zyk, N. V. *Russ. Chem. Rev.* **2005**, *74*, 531−553 and references cited therein.
(3) Chirik, P. J.; Wieghardt, K. *Science* **2010**, *327*, 794−795.
(4) Dzik, W. I.; van der Vlugt, J. I.; Reek, J. N. H.; de Bruin, B. *Angew. Chem., Int. Ed.* **2011**, *50*, 3356−3358.
(5) Lyaskovskyy, V.; de Bruin, B. *ACS Catal.* **2012**, *2*, 270−279.
(6) Grützmacher, H. *Angew. Chem., Int. Ed.* **2008**, *47*, 1814−1818.
(7) Forum Issue on Redox Noninnocent Ligands: . *Inorg. Chem.* **2011**, *50*, 9737.
(8) (a) Kaim, W. *Dalton Trans.* **2003**, 761−768. (b) Kaim, W.; Schwederski, B. *Coord. Chem. Rev.* **2010**, *254*, 1580−1588.
(9) (a) Chaudhuri, P.; Hess, M.; Flörke, U.; Wieghardt, K. *Angew. Chem., Int. Ed.* **1998**, *37*, 2217−2220. (b) Chaudhuri, P.; Hess, M.; Müller, J.; Hildenbrand, K.; Bill, E.; Weyhermüller, T.; Wieghardt, K. *J. Am. Chem. Soc.* **1999**, *121*, 9599−9610. (c) Mukherjee, C.; Pieper, U.; Bothe, E.; Bachler, V.; Bill, E.; Weyhermüller, T.; Chaudhuri, P. *Inorg. Chem.* **2008**, *47*, 8943−8956.
(10) Luca, O. R.; Crabtree, R. H. *Chem. Soc. Rev.* **2013**, *42*, 1440−1459.
(11) (a) Sadler, J. L.; Bard, A. J. *J. Am. Chem. Soc.* **1968**, *90*, 1979−1989. (b) Ghosh, B. K.; Chakravorty, A. *Coord. Chem. Rev.* **1989**, *95*, 239−294. (c) Pal, C. K.; Chattopadhyay, S.; Sinha, C. R.; Chakravorty, A. *Inorg. Chem.* **1996**, *35*, 2442−2447. (d) Misra, T. K.; Das, D.; Sinha, C. R.; Ghosh, P.; Pal, C. K. *Inorg. Chem.* **1998**, *37*, 1672−1678 and references cited therein.
(12) Doslik, N.; Sixt, T.; Kaim, W. *Angew. Chem., Int. Ed.* **1998**, *37*, 2403−2404.
(13) Shivakumar, M.; Pramanik, K.; Ghosh, P.; Chakravorty, A. *Chem. Commun.* **1998**, 2103.
(14) (a) Samanta, S.; Ghosh, P.; Goswami, S. *Dalton Trans.* **2012**, *41*, 2213−2226. (b) Paul, N. D.; Rana, U.; Goswami, S.; Mondal, T. K.; Goswami, S. *J. Am. Chem. Soc.* **2012**, *134*, 6520−6523. (c) Joy, S.; Krämer, T.; Paul, N. D.; Banerjee, P.; McGrady, J. E.; Goswami, S. *Inorg. Chem.* **2011**, *50*, 9993−10004. (d) Paul, N.; Samanta, S.; Goswami, S. *Inorg. Chem.* **2010**, *49*, 2649−2655. (e) Sanyal, A.; Chatterjee, S.; Castiñeiras, A.; Sarkar, B.; Singh, P.; Fiedler, J.; Záliš, S.; Kaim, W.; Goswami, S. *Inorg. Chem.* **2007**, *46*, 8584−8593. (f) Sanyal, A.; Banerjee, P.; Lee, G.-H.; Peng, S.-M.; Hung, C.-H.; Goswami, S. *Inorg. Chem.* **2004**, *43*, 7456−7462. (g) Samanta, S.; Singh, P.; Fiedler, J.; Záliš, S.; Kaim, W.; Goswami, S. *Inorg. Chem.* **2008**, *47*, 1625−1633.
(15) (a) Kaim, W. *Inorg. Chem.* **2011**, *50*, 9752−976. (b) Sarkar, B.; Patra, S.; Fiedler, J.; Sunoj, R. B.; Janardana, D.; Mobin, S. M.; Niemeyer, M.; Lahiri, G. K.; Kaim, W. *Angew. Chem., Int. Ed.* **2005**, *44*, 5655−5658. (c) Sarkar, B.; Patra, S.; Fiedler, J.; Sunoj, R. B.; Janardanan, D.; Lahiri, G. K.; Kaim, W. *J. Am. Chem. Soc.* **2008**, *130*, 3532−3542. (d) Kaim, W. *Coord. Chem. Rev.* **2001**, *219*−*221*, 463−488.
(16) (a) Shivakumar, M.; Pramanik, K.; Ghosh, P.; Chakravorty, A. *Inorg. Chem.* **1998**, *37*, 5968−5969. (b) Pramanik, K.; Shivakumar, M.; Ghosh, P.; Chakravorty, A. *Inorg. Chem.* **2000**, *39*, 195−199.
(17) (a) Venkataramani, S.; Jana, U.; Dommaschk, M.; Sönnichsen, F. D.; Tuczek, F.; Herges, R. *Science* **2011**, *331*, 445−448. (b) Braunstein, P.; Naud, F. *Angew. Chem., Int. Ed.* **2001**, *40*, 680−699. (c) van der Vlugt, J. I.; Reek, J. N. H. *Angew. Chem., Int. Ed.* **2009**, *48*, 8832−8846.
(18) (a) Li, Y.; Lin, Z.-Y.; Wong, W.-T. *Eur. J. Inorg. Chem.* **2001**, 3163−3173. (b) Deibel, N.; Schweinfurth, D.; Hohloch, S.; Sarkar, B. *Inorg. Chim. Acta* **2012**, *380*, 269. (c) Chand, B. G.; Ray, U. S.; Mostafa, G.; Cheng, J.; Lu, T.-H.; Sinha, C. *Inorg. Chim. Acta* **2005**, *358*, 1927−1933. (d) Saha (Halder), S.; Chand, B. G.; Wu, J.-S.; Lu, T.-H.; Raghavaiah, P.; Sinha, C. *Polyhedron* **2012**, *46*, 81−89.
(19) Dougan, S. J.; Melchart, M.; Habtemariam, A.; Parsons, S.; Sadler, P. J. *Inorg. Chem.* **2006**, *45*, 10882−10894.
(20) Holm, R. H.; Cotton, F. A. *J. Chem. Phys.* **1960**, *32*, 1168−1172.
(21) (a) Min, K. S.; DiPasquale, A. G.; Rheingold, A. L.; white, H. S.; Miller, J. S. *J. Am. Chem. Soc.* **2009**, *131*, 6229−6236. (b) Duggan, D. M.; Hendrickson, D. N. *Inorg. Chem.* **1975**, *14*, 1944−1956. (c) Brewer, G.; Sinn, E. *Inorg. Chem.* **1985**, *24*, 4580−4584. (d) Tandon, S. S.; Thompson, L. K.; Bridson, J. N.; Dewan, J. C. *Inorg. Chem.* **1994**, *33*, 54−61. (e) Glerup, J.; Goodson, P. A.; Hodgson, D. J.; Michelsen, K. *Inorg. Chem.* **1995**, *34*, 6255−6264.
(22) Santra, B. K.; Lahiri, G. K. *J. Chem. Soc., Dalton Trans.* **1998**, 139−145.
(23) Johnson, E. C.; Sullivan, B. P.; Salmon, D. J.; Adeyemi, S. A.; Meyer, T. J. *Inorg. Chem.* **1978**, *17*, 2211−2215.
(24) (a) Lu, C. C.; Weyhermüller, T.; Bill, E.; Wieghardt, K. *Inorg. Chem.* **2009**, *48*, 6055−6064. (b) Lu, C. C.; Bill, E.; Weyhermüller, T.; Bothe, E.; Wieghardt, K. *J. Am. Chem. Soc.* **2008**, *130*, 3181−3197.
(25) Miller, J. S.; Min, K. S. *Angew. Chem., Int. Ed.* **2009**, *48*, 262−272.
(26) de Bruin, B.; Bill, E.; Bothe, E.; Weyhermüller, T.; Wieghardt, K. *Inorg. Chem.* **2000**, *39*, 2936−2947.
(27) Goswami, S.; Mukherjee, R. N.; Chakravorty, A. *Inorg. Chem.* **1983**, *22*, 2825−2832.
(28) Campbell, N.; Henderson, A. W.; Taylor, D. *J. Chem. Soc.* **1953**, 1281−1285.
(29) Priewisch, B.; Rück-Braun, K. *J. Org. Chem.* **2005**, *70*, 2350−2352.

(30) (a) Sheldrick, G. M. *Acta Crystallogr., Sect. A* **1990**, *46*, 467−473. (b) Sheldrick, G. M. *SHELXL 97, Program for the refinement of crystal structures*; University of Göttingen: Göttingen, Germany, 1997.
(31) Frisch, M. J.; Trucks, G. W.; Schlegel, H. B.; Scuseria, G. E.; Robb, M. A.; Cheeseman, J. R.; Montgomery, J. A., Jr.; Vreven, T.; Kudin, K. N.; Burant, J. C.; Millam, J. M.; Iyengar, S. S.; Tomasi, J.; Barone, V.; Mennucci, B.; Cossi, M.; Scalmani, G.; Rega, N.; Petersson, G. A.; Nakatsuji, H.; Hada, M.; Ehara, M.; Toyota, K.; Fukuda, R.; Hasegawa, J.; Ishida, M.; Nakajima, T.; Honda, Y.; Kitao, O.; Nakai, H.; Klene, M.; Li, X.; Knox, J. E.; Hratchian, H. P.; Cross, J. B.; Bakken, V.; Adamo, C.; Jaramillo, J.; Gomperts, R.; Stratmann, R. E.; Yazyev, O.; Austin, A. J.; Cammi, R.; Pomelli, C.; Ochterski, J. W.; Ayala, P. Y.; Morokuma, K.; Voth, G. A.; Salvador, P.; Dannenberg, J. J.; Zakrzewski, V. G.; Dapprich, S.; Daniels, A. D.; Strain, M. C.; Farkas, O.; Malick, D. K.; Rabuck, A. D.; Raghavachari, K.; Foresman, J. B.; Ortiz, J. V.; Cui, Q.; Baboul, A. G.; Clifford, S.; Cioslowski, J.; Stefanov, B. B.; Liu, G.; Liashenko, A.; Piskorz, P.; Komaromi, I.; Martin, R. L.; Fox, D. J.; Keith, T.; Al-Laham, M. A.; Peng, C. Y.; Nanayakkara, A.; Challacombe, M.; Gill, P. M. W.; Johnson, B.; Chen, W.; Wong, M. W.; Gonzalez, C.; Pople, J. A. *Gaussian 09*, revision A.02; Gaussian, Inc.: Wallingford, CT, 2004.
(32) (a) Becke, A. D. *J. Chem. Phys.* **1993**, *98*, 5648−5652. (b) Lee, C.; Yang, W.; Parr, R. G. *Phys. Rev. B: Condens. Matter Mater. Phys.* **1988**, *37*, 785−789. (c) Vosko, S. H.; Wilk, L.; Nusair, M. *Can. J. Phys.* **1980**, *58*, 1200−1211. (d) Stephens, P. J.; Devlin, F. J.; Chabalowski, C. F.; Frisch, M. J. *J. Phys. Chem.* **1994**, *98*, 11623−11627.
(33) Schäfer, A.; Huber, C.; Ahlrichs, R. *J. Chem. Phys.* **1994**, *100*, 5829−5835.
(34) Schäfer, A.; Horn, H.; Ahlrichs, R. *J. Chem. Phys.* **1992**, *97*, 2571−2577.
(35) Ginsberg, A. P. *J. Am. Chem. Soc.* **1980**, *102*, 111−117.
(36) (a) Noodleman, L.; Case, D. A.; Aizman, A. *J. Am. Chem. Soc.* **1988**, *110*, 1001−1005. (b) Noodleman, L.; Davidson, E. R. *Chem. Phys.* **1986**, *109*, 131−143. (c) Noodleman, L.; Norman, J. G., Jr.; Osborne, J. H.; Aizman, C.; Case, D. A. *J. Am. Chem. Soc.* **1985**, *107*, 3418−3426. (d) Noodleman, L. *J. Chem. Phys.* **1981**, *74*, 5737−5743.
(37) Mulliken, R. S. *J. Chem. Phys.* **1955**, *23*, 1833−1840.